

# The application of microwaves in the synthesis of $\text{Ce}_{0.9}\text{Pr}_{0.1}\text{O}_2$ nanostructured powders

Federica Bondioli,<sup>\*a</sup> Anna M. Ferrari,<sup>b</sup> Cristina Leonelli,<sup>b</sup> Cristina Siligardi,<sup>b</sup> Neil A. Hart<sup>c</sup> and Nigel G. Evans<sup>d</sup>

<sup>a</sup>Department of Materials and Environmental Engineering, Faculty of Engineering, University of Modena, Via Vignolese 905/c, 41100 Modena, Italy. Tel: +39-059-2056235;

Fax: +39-59-2056243

<sup>b</sup>Department of Chemistry, Faculty of Engineering, University of Modena, Via Campi 183, 41100 Modena, Italy. E-mail: fedebond@unimo.it

<sup>c</sup>School of Engineering, Staffordshire University, Beaconside, Stafford, UK ST18 0AD

<sup>d</sup>Petrie Technologies Ltd, Ackhurst Road, Chorley, Lancs., UK PR7 1NH

Received 8th May 2001, Accepted 18th July 2001

First published as an Advance Article on the web 7th September 2001

In this work  $\text{Ce}_{0.9}\text{Pr}_{0.1}\text{O}_2$  powders were synthesised by the coprecipitation method starting from a solution of the cation nitrates. The possible use of microwave technology in both drying and calcination steps was evaluated. XRD analysis, dielectric properties measurements, and colour characterisation were used in order to determine the benefits of using microwaves.

## Introduction

Ceria ( $\text{CeO}_2$ ) has been considered a useful material and attracted interest for use in catalytic supports (for automotive exhaust systems).<sup>1,2</sup> Several rare-earth-doped cerium oxides exhibit high oxygen ion conductivity which makes them interesting materials for applications as solid electrolytes in solid oxide fuel cells.<sup>3,4</sup> Ceria has a fluorite structure that is stable from room temperature to its melting point ( $\sim 2600^\circ\text{C}$ ) as compared with other pure oxides with oxygen ion conductivity, zirconia and bismuth oxide, which show polymorph transformations in different temperature ranges. Ceria has also received attention for other various applications such as additives for glass and glazes, stabilizers for  $\text{ZrO}_2$ , and as a glass polish, for which the use of nanocrystalline powders is an important factor. Several techniques including hydrothermal synthesis,<sup>5-8</sup> urea-based homogeneous precipitation,<sup>9-12</sup> hexamethylenetetramine-based homogeneous precipitation,<sup>13,14</sup> coprecipitation,<sup>15,16</sup> decomposition of oxalate precursors,<sup>17</sup> forced hydrolysis,<sup>18</sup> and electrochemical synthesis<sup>19</sup> have been developed for the production of ceria or cation-doped ceria particles and their precursors. However little effort has been directed at the preparation of ultra-fine particles in aqueous solution through microwave irradiation.<sup>20</sup> The use of microwaves could offer many benefits in the form of cost saving through the reduction in processing time and energy input and may result in products which are either not formed or only produced in low yield by the corresponding conventional methods.<sup>21,22</sup> Direct and rapid sample heating by microwave radiation initiates reactions uniformly and may even drive reactions along different kinetic pathways.<sup>23,24</sup> Consequently, it is possible that microwave heating could offer improved yields of target compounds or open up new synthesis routes entirely.

In this paper we report on the application of microwave technology to coprecipitation synthesis in the  $\text{Ce}_{0.9}\text{Pr}_{0.1}\text{O}_2$  system.<sup>25</sup> In particular, this work focuses on the possibility of microwave heating in both drying and calcination steps of praseodymia/ceria coprecipitated precursors. The properties of the powders produced are compared with those of traditionally obtained powders with the aim of explaining the formation

mechanism of the structure, synthesis temperature, stability, and colour quality.

## Experimental procedure

### Sample preparation

Powders containing 10 mol% of praseodymium were obtained from cerium(IV) ammonium nitrate ( $(\text{NH}_4)_2\text{Ce}(\text{NO}_3)_2$ , RPE Carlo Erba, Milan, Italy) and praseodymium(III) nitrate ( $\text{Pr}(\text{NO}_3)_3 \cdot 6\text{H}_2\text{O}$ , RPE Carlo Erba, Milan, Italy) by raising the pH of the solution to 9 with ammonia ( $\text{NH}_3(\text{aq})$ , RPE Carlo Erba, Milan, Italy). To evaluate the effect of praseodymium on the physical and chemical properties, samples of pure ceria and pure praseodymia were also prepared using the same chemicals. Gels were washed and then dried in a commercial microwave oven (CEM Co., MAS 7000, NC, USA, 2.45 GHz, 1 kW) and in a conventional oven, respectively. The dried powder samples obtained were calcined in air in either a microwave furnace or in a conventional electric oven at a range of temperatures from 300 to 1200 °C. Both microwave and conventional ovens were preheated to the processing temperature before the powder samples were inserted. The temperature was measured in each case using identical metal sheathed thermocouples placed in close proximity to the sample. Once the treatment temperature was reached in both furnaces, samples were inserted for 15 min. Samples were then removed and air cooled to room temperature.

### Powder characterisation

In order to understand the mechanism of microwave firing and to consider the effect of praseodymium in a microwave field, measurements of dielectric properties at elevated temperatures were made on ceria, praseodymia and 10% praseodymia/ceria dried gels using the cavity perturbation method.<sup>26,27</sup> Samples were measured at 2.45 GHz from room temperature to 1400 °C at 100 °C intervals. The data were compared with the thermal behaviour of the samples as obtained by thermogravimetry (TG), and differential thermal analysis (DTA), in air at a heating rate of 20 °C min<sup>-1</sup>, using simultaneous TG/DTA equipment (Netzsch, STA 409, Selb, Germany).

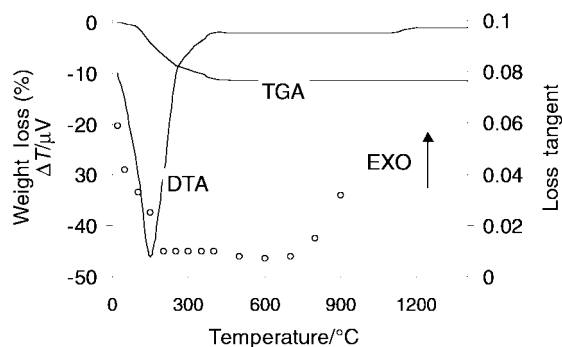


Fig. 1 TGA, DTA and loss tangent (○) curves vs. temperature for the pure ceria dried gel.

To investigate the structure and crystallinity after thermal treatment, the calcined powders were analysed with a Philips PW 3710 computer-assisted X-ray (Cu-K $\alpha$ ) powder diffractometer (XRD). The XRD patterns were collected in the range  $2\theta$  20–70° at room temperature. The scanning rate was 0.004° s<sup>-1</sup>, with a step size of 0.02°. The mean value of the crystallite size was estimated from diffraction peak broadening using the Sherrer formula.<sup>28</sup>

The determination of specific surface areas was made experimentally using multipoint BET theory<sup>29</sup> (Micromeritics, Gemini 2360, USA). Particle sizes were also calculated from the specific surface area data,<sup>30</sup> using the theoretical density of ceria (7.184 g cm<sup>-3</sup>).<sup>6</sup>

To confirm that solid solution formation had taken place, leaching tests in boiling solutions of concentrated (36 mass%) hydrochloric acid were performed.<sup>31</sup> The Pr content of the solutions was determined by ICP-AES spectroscopy (Varian, Liberty 200, Australia).

To verify the nature and microstructure of samples after the different processing steps, scanning electron microscopy (SEM) observations were performed (Philips, XL 40, The Netherlands). Finally, to investigate the colour of the red pigments, samples were analysed with a UV-Vis spectrophotometer with analytical software for colour measurements (Perkin Elmer, Lambda 19, Norwalk, CT, USA).

## Results and discussion

### Thermal and dielectric properties

Fig. 1 shows the loss tangent and the DTA/TG curves vs. temperature plot for the pure ceria dried powder. At low temperature, the powder readily absorbs microwave energy since it contains a high concentration of OH<sup>-</sup> groups but this effect decreases at 200 °C. At about 600 °C there is a rise in the loss tangent suggesting thermally activated conductivity. The linear nature of the permittivity response and its apparently negative temperature coefficient (Fig. 2) suggests that the

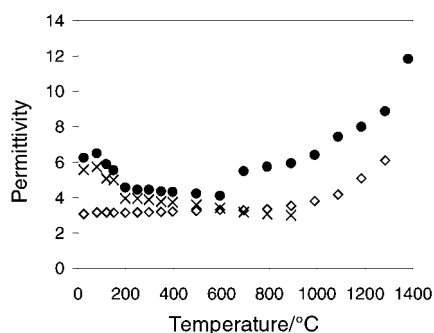


Fig. 2 Permittivity vs. temperature curves for ceria (×), praseodymia (◇) and 10% praseodymia/ceria gel (●).

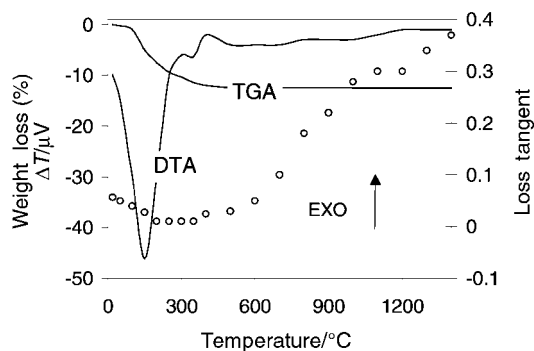


Fig. 3 TGA, DTA and loss tangent (○) curves vs. temperature of the Pr-doped dried gel.

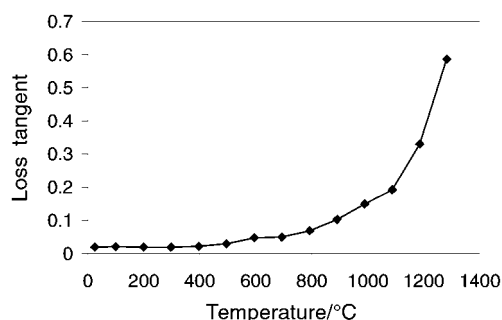


Fig. 4 Loss tangent curve vs. temperature of a pure praseodymia dried gel.

polarisation mechanisms present are electron cloud deformation and ion-ion polarisability (change in mean spacing of the anion and cation sublattice) A marked increase in permittivity with temperature at about 800 °C indicates that for both praseodymia and 10% praseodymia/ceria gel (Fig. 2), an ion jump relaxation mechanism was present.

Fig. 3 shows the loss tangent and thermal data of ceria gel coprecipitated with 10 mol% praseodymium ions. The behaviour is similar to ceria precipitated powders but the presence of praseodymium significantly increases the dielectric loss of the sample above 300 °C. This effect is due to the fact that praseodymium oxide shows a marked increase in loss tangent compared with pure and Pr-doped ceria samples (Fig. 4). The sharp exothermic peak in the DTA curve at about 450 °C, with no related weight loss, is probably due to the formation of the solid solution.<sup>32</sup>

The Arrhenius plots shown in Fig. 5 are obtained by assuming that conductivity  $\sigma$  is the predominant loss mechanism. The conductivity is defined by eqn. (1):

$$\sigma = 2f\pi\epsilon_0\epsilon'' \quad (1)$$

where  $f$  = frequency (GHz),  $\epsilon_0 = 8.854 \times 10^{-12}$  (F m<sup>-1</sup>) and  $\epsilon''$  = loss factor.

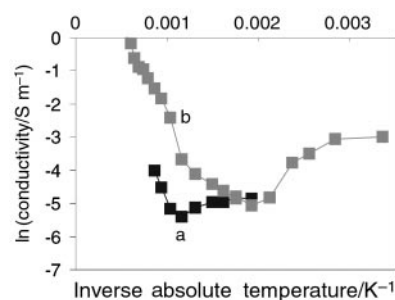


Fig. 5 Arrhenius plots of ln conductivity vs. inverse absolute temperature for ceria (a) and 10% praseodymia/ceria (b) systems.

For thermally activated conductivity, eqn. (2) holds:

$$\sigma = \sigma_0 e^{(E/kT)} \quad (2)$$

where  $\sigma_0$  is a constant,  $k$  is the Boltzmann constant ( $1.38 \times 10^{-23} \text{ J K}^{-1}$ ) and  $E$  is the activation energy. Taking natural logs and rearranging, a line with slope  $E/K$  is obtained (Fig. 5).

From these data, the activation energy of ceria gel is 0.58 eV ( $0.93 \times 10^{-19} \text{ J}$ ) while that of the 10% praseodymia/ceria composition is 0.48 eV ( $0.77 \times 10^{-19} \text{ J}$ ), confirming that praseodymia improves the kinetic parameters in the microwave field.

### Characterisation of powders

The resulting microwave-dried powder was homogeneous and not agglomerated and its particle size was  $<1 \mu\text{m}$ ; the measured specific surface area was about  $237 \text{ m}^2 \text{ g}^{-1}$ .

The microwave drying process took only a few minutes which is a substantial improvement over traditional methods which take up to 5 hours.

Additionally, microwave drying resulted in the formation of a less dense powder when compared with a conventionally dried sample. The powder was therefore more easily broken down during the subsequent grinding process. This behaviour reproduces fairly well that of  $\text{Al}_2\text{O}_3\text{-Cr}_2\text{O}_3$  compositions presented elsewhere by us.<sup>33,34</sup>

The microwave drying process does not induce any changes to the powders. As with conventionally dried samples,<sup>25</sup> XRD patterns of the microwave-dried powders show all the major reflections of the  $\text{CeO}_2$  fluorite structure.

To investigate the nature of the samples after microwave calcination over the temperature range 300–1200 °C, all heat-treated 10% praseodymia/ceria samples were subjected to powder X-ray diffraction measurements. The patterns showed the same crystalline structure for all calcination temperatures used. All of the peaks were attributed to crystalline cerium oxide,  $\text{CeO}_2$ , with a cubic fluorite structure (ICDD file 34-394). Comparison of the spectra shows that the crystallinity increases with the calcination temperature (Fig. 6) as indicated by both increasing intensity and sharpening of the peaks.

This trend was also confirmed by the average dimension of the primary and secondary particles, as determined using the Sherrer formula from the XRD patterns and by BET data manipulation, respectively (Fig. 7). This data suggests a progressive grain growth and successive agglomeration with increasing temperature, in particular crystallite size values are similar to those of the powder particles up to 700 °C. At higher temperatures these values diverge slightly as a consequence of a possible formation of agglomerates of primary particles. In order to verify this observation, a microstructural investigation has been performed by SEM. Fig. 8(a) clearly confirms that the powders obtained at 1000 °C are constituted of agglomerates of 0.1–0.2  $\mu\text{m}$  sized primary particles.

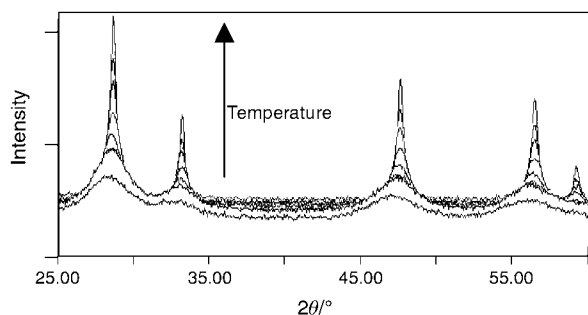


Fig. 6 XRD patterns of 10% praseodymia/ceria samples as a function of microwave temperature.

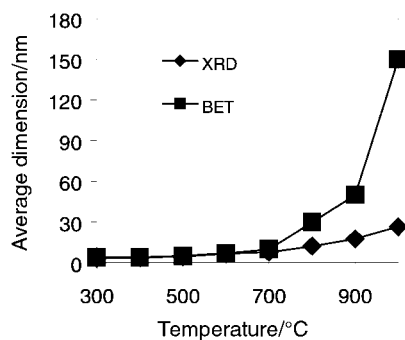


Fig. 7 Correlation between the data obtained by both XRD ( $\pm 0.1 \text{ nm}$ ) and BET ( $\pm 0.1 \text{ nm}$ ) data manipulation for microwave calcined 10% praseodymia/ceria powders).

Conversely, the powders obtained through conventional heating exhibit remarkably higher dimensions due to growth and sintering processes. This behaviour is also suggested by the coalescence and formation of hard aggregates illustrated by the SEM images shown in Fig. 8(b).

The XRD patterns did not clearly define the condition of the solid solution formation since the major reflection peaks,  $3.12_{10}$ ,  $1.91_5$ ,  $1.63_4$  and  $3.11_{10}$ ,  $1.91_7$ ,  $1.63_6 \text{ \AA}$ , corresponding to  $\text{CeO}_2$  and  $\text{PrO}_2$ , respectively, are overlapped. Leaching tests carried out with a boiling solution of concentrated (36 mass%) hydrochloric acid were used to evaluate solid solution formation, the effective diffusion of praseodymium in the ceria lattice and the stability of the obtained powders. This selective chemical attack allows the amount of unreacted soluble praseodymium oxides ( $\text{Pr}_6\text{O}_{11}$ ,  $\text{Pr}_2\text{O}_3$  and  $\text{PrO}_2$ ) to be determined. The lower the percentage of cation release, the greater the extent of solid solution formation. Fig. 9 illustrates that greater product formation, associated with a lower praseodymium leaching, is found in samples obtained through microwave treatment at 800 °C. These results are consistent with the change in the dielectric properties of the mixed

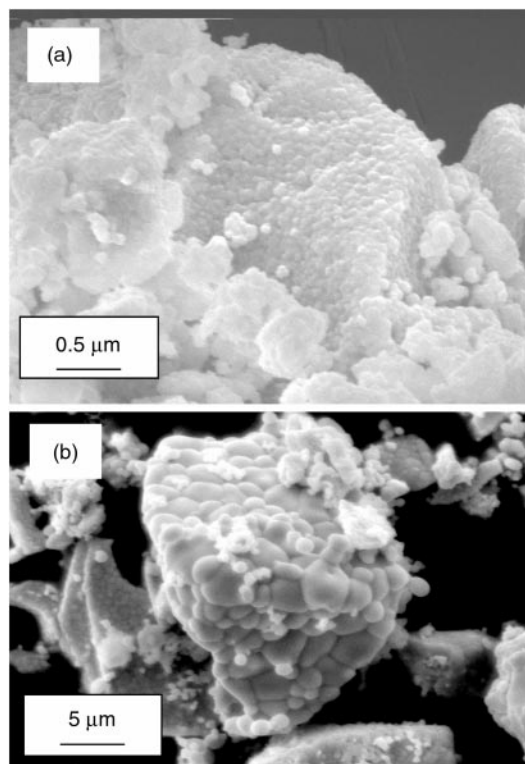


Fig. 8 SEM micrographs of 10% praseodymia/ceria samples treated at 1000 °C for 15 min. (a) Microwave (10000 $\times$ ) and (b) traditionally (3500 $\times$ ) calcined powders

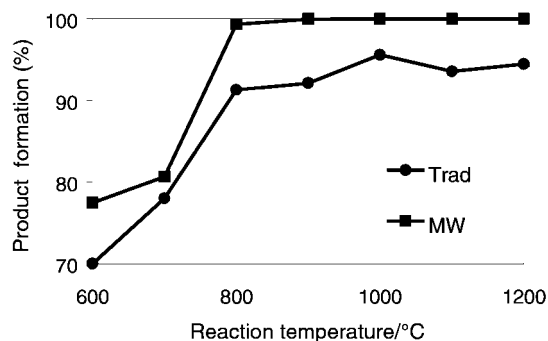


Fig. 9 Product formation (%) (measured by leaching) in coprecipitated powders obtained by microwave and traditional heating (15 min).

hydroxides as a function of temperature, which show an increase in loss tangent at 700 °C indicating a possible coupling mechanism (Fig. 3). Fig. 9 clearly shows that conventional heating fails to result in production of a 10% praseodymia/ceria solid solution for temperatures up to 1200 °C.

According to Jørgensen and Rittershaus,<sup>35</sup> the red colour of the praseodymium-doped samples, corresponding to powders with a strong absorption for  $\lambda < 600$  nm, is related to a charge-transfer band due to an electron transfer from the ligand orbitals to the praseodymium cation. There are several methods for colour measurements, but it is accepted industrial practice to specify the colour of a pigment using the CIE-Lab method.<sup>36</sup> The colour measurements (see Table 1) showed systematic changes in the CIE-Lab parameters correlating directly with the structural alterations of the solid solutions as a function of the heating method used, and of the calcination temperature.  $L^*$  values indicate that the degree of darkness of powder samples which decreases with increasing calcination temperature and reaches a maximum value for microwave calcination at 800 °C. Above this temperature the value of  $L^*$  remains almost constant. The behavior of the  $a^*$  parameter, representing a scale extending from green ( $-a^*$ ) to red ( $+a^*$ ), follows the same pattern as that of the  $L^*$  parameter.

The results obtained also show how the powders prepared by microwave calcination develop higher red shades at all temperatures investigated. The lower  $a^*$  values may be explained by considering the incomplete solubilization of two oxides, as confirmed by ICP-AES results. These data are not affected by the different grain size of the powders obtained through microwave or traditional heat treatments. If changes were due to the increase in surface area of the microwave calcined powders, the  $L^*$  parameter should have shown an increase, while the  $a^*$  parameter should have shown a decrease in value, when compared to traditionally calcined powders. In fact the opposite trend shows how significant the effect of microwave processing is on the solid solution formation.

However, for reddish colours, with a complex relationship between  $L^*$  and  $a^*$  values, there are some difficulties, and more understandable and usable information can be obtained by

Table 1 Colour parameters ( $L^*$  and  $a^*$ ) of the coprecipitated powders obtained at different temperatures by microwave and traditional treatments

Temperature/°C	$L^*$		$a^*$	
	MW	Traditional	MW	Traditional
700	55.2	48.2	8.2	1.8
800	57.2	50.1	9.8	2.2
900	57.2	49.8	9.9	2.8
1000	57.8	52.3	10.1	3.1
1100	57.9	53.2	9.8	3.6
1200	57.8	54.8	10	3.8

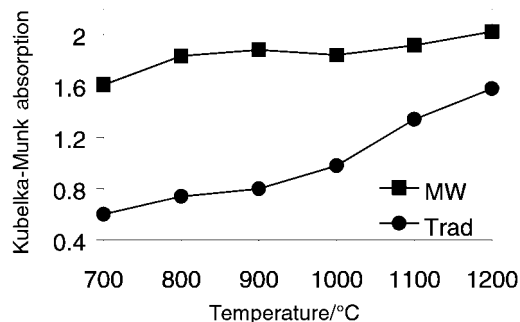


Fig. 10 Kubelka–Munk parameter vs. temperature and heating treatment used.

using the Kubelka–Munk absorption function, obtained from the reflection spectra.<sup>37</sup> The Kubelka–Munk data confirmed the results obtained from leaching tests (Fig. 10). In particular, the powders obtained by microwave calcination reach a maximum absorption at the wavelength plotted (560 nm) by 800 °C. The successive increase of this value with increasing calcination temperature can be correlated to the increase in the mean size of the powders. For the powders obtained using the traditional processing method, the absorption intensity is always below the values obtained for the microwave calcined powders across the range of calcination temperatures used.

## Conclusion

Nanostructured  $\text{Ce}_{0.9}\text{Pr}_{0.1}\text{O}_2$  (ss) powders have been synthesized via the coprecipitation route. The application of microwaves in both drying and calcination processes of coprecipitated powders seems to be an efficient method to improve powder quality, leading to shorter processing schedules and enhanced colour development. The dielectric property data showed that the presence of praseodymium increases the loss factor of ceria precursors by approximately one order of magnitude, while the linear response of  $\log \epsilon''$  with temperature indicated that conductivity is the predominant loss mechanism.

## Acknowledgements

The financial support given by M.U.R.S.T.-PRIN contract, “Application of the microwave technology to physico-chemical processing involving solids: 1999–2000” is gratefully acknowledged.

## References

- P. Fornasiero, G. Balducci, R. Di Monte, J. Kaspar, V. Sergo, G. Gubitosa, A. Ferrero and M. Graziani, *J. Catal.*, 1996, **164**, 173.
- G. Ranga Rao, P. Fornasiero, R. Di Monte, J. Kaspar, G. Vlaic, G. Balducci, S. Meriani, G. Gubitosa, A. Cremona and M. Graziani, *J. Catal.*, 1996, **162**, 1.
- T. Kudo and H. Obayashi, *J. Electrochem. Soc.*, 1975, **122**(1), 42.
- H. Yahiro, Y. Baba, K. Eguchi and H. Arai, *J. Electrochem. Soc.*, 1988, **135**(8), 2077.
- E. Tani, M. Yoshimura and S. Somyia, *J. Mater. Sci. Lett.*, 1982, **1**, 461.
- Y. C. Zhou and M. N. Rahaman, *J. Mater. Res.*, 1993, **8**(7), 1680.
- M. Hirano and E. Kato, *J. Mater. Sci. Lett.*, 1996, **15**, 1249.
- M. Hirano and E. Kato, *J. Am. Ceram. Soc.*, 1996, **79**(3), 777.
- E. Matijevic and W. P. Hsu, *J. Colloid Interface Sci.*, 1987, **118**, 506.
- X. Chu, W. Chung and L. D. Schmidt, *J. Am. Ceram. Soc.*, 1993, **76**(8), 2115.
- M. Akinc and D. Sordelet, *Adv. Ceram. Mater.*, 1987, **2**(3A), 232.
- B. Aiken, W. P. Hsu and E. Matijevic, *J. Am. Ceram. Soc.*, 1988, **71**(10), 845.
- P. L. Chen and I.-W. Chen, *J. Am. Ceram. Soc.*, 1993, **76**(10), 845.
- P. L. Chen and I.-W. Chen, *J. Am. Ceram. Soc.*, 1993, **79**(12), 3129.

- 15 H. Yahiro, Y. Baba, K. Eguchi and H. Arai, *J. Electrochem. Soc.*, 1988, **135**, 2077.
- 16 T. J. Kirk and J. Winnick, *J. Electrochem. Soc.*, 1993, **140**, 3494.
- 17 J. V. Herle, T. Horita, T. Kawada, N. Sakai, H. Yokokawa and M. Dokiya, *J. Am. Ceram. Soc.*, 1997, **80**(4), 933.
- 18 W. P. Hsu, L. Ronnquist and E. Matijevic, *Langmuir*, 1988, **4**, 31.
- 19 Y. Zhou, R. J. Philips and J. A. Switzer, *J. Am. Ceram. Soc.*, 1995, **78**(4), 981.
- 20 D. Daichuan, H. Pinjie and D. Shushan, *Mater. Res. Bull.*, 1995, **30**, 531.
- 21 D. R. Baghurst, R. C. B. Copley, H. Fleischer, D. M. P. Mingos, G. O. Kyd, L. J. Yellowlees, A. J. Welch, T. R. Spalding and D. O'Connell, *J. Organomet. Chem.*, 1993, **447**, C14.
- 22 D. A. C. Stuerger, K. Gonon and M. Lallemand, *Tetrahedron*, 1993, **49**, 6229.
- 23 D. A. C. Stuerger and P. Gaillard, *J. Microwave Power Electromagn. Energy*, 1996, **31**, 87.
- 24 D. A. C. Stuerger and P. Gaillard, *J. Microwave Power Electromagn. Energy*, 1996, **31**, 101.
- 25 F. Bondioli, A. B. Corradi, T. Manfredini, C. Leonelli and R. Bertocello, *Chem. Mater.*, 2000, **12**(2), 324.
- 26 M. Arai, J. G. P. Binner, A. L. Bowden, T. E. Cross, N. G. Evans, M. G. Hamlyn, R. Hutcheon, G. Morin and B. Smith, *Ceram. Trans.*, 1993, **36**, 539.
- 27 R. M. Hutcheon, M. de Jong, F. Adams, G. Wood, J. MacGregor and B. Smith, *J. Microwave Power*, 1992, **27**(2), 93.
- 28 P. Klug and L. E. Alexander, in *X-Ray Diffraction Procedure*, Wiley, New York, 1954, ch. 9.
- 29 L. Svarovsky, in *Powder Testing Guide: Methods of Measuring the Physical Properties of Bulk Powders*. Published on behalf of the British Materials Handling Board by Elsevier Applied Science, London and New York, 1987.
- 30 K. Kodera, in *Powders (Theory and Applications)*, ed. K. Kubo, E. Suito, Y. Nakagawa and S. Hayakawa, Maruzen, Tokyo, Japan, 1962.
- 31 F. Bondioli, A. M. Ferrari, C. Leonelli and T. Manfredini, *Mater. Res. Bull.*, 1998, **33**(5), 723.
- 32 B. Xia, L. Duan and Y. Xie, *J. Am. Ceram. Soc.*, 2000, **83**(5), 1077.
- 33 F. Bondioli, A. M. Ferrari, C. Leonelli, C. Siligardi and T. Manfredini, *Ceram. Trans.*, 1997, **80**, 483.
- 34 F. Bondioli, A. B. Corradi, A. M. Ferrari, C. Leonelli, C. Siligardi, T. Manfredini and N. G. Evans, *J. Microwave Power Electromagn. Energy*, 1998, **33**(1), 18.
- 35 C. K. Jørgensen and E. Rittershaus, *Mater. Fys. Medd. K. Dan. Vidensk. Selsk.*, 1967, **35**, 15.
- 36 R. S. Hunter, *J. Opt. Soc. Am.*, 1958, **48**, 985.
- 37 D. R. Eppler and R. A. Eppler, *Ceram. Eng. Sci. Proc.*, 1996, **17**(1), 77.